

## Perspective

### The Preorganization Step in Organic Reaction Mechanisms. Charge-Transfer Complexes as Precursors to Electrophilic Aromatic Substitutions

Sergiy V. Rosokha and Jay K. Kochi\*

Department of Chemistry, University of Houston, Houston, Texas 77204-5003

*jkochi@mail.uh.edu*

Received November 14, 2001

Metastable (pre-reactive) intermediates, as commonplace transients in simple bimolecular reactions, are usually unobserved (and ignored)—though they provide vital mechanistic insight. Thus, the preequilibrium (charge-transfer) complexes of various aromatic donors with rather typical electron acceptors such as Br<sub>2</sub>, NO<sup>+</sup>, and NO<sub>2</sub><sup>+</sup> are examined quantitatively (via their molecular and electronic structures) to reveal surprisingly unorthodox aspects of what is conventionally referred to in organic chemistry textbooks as electrophilic aromatic bromination, nitrosation, and nitration, respectively.

#### Introduction

The earliest mechanistic formulations of bimolecular reactions, both in solution and gas phase, have included the preequilibrium formation of a metastable (1:1) complex as an important (initial) encounter.<sup>1,2</sup> Although such a preorganization step is also considered critical in formulating biochemical mechanisms (e.g., enzyme/substrate complexes, antibody/antigen binding, etc.<sup>3</sup>), it has heretofore not played a comparable role in the formulation of organic reaction mechanisms—as readily apparent by even a cursory inspection of any contemporary organic chemistry textbook.

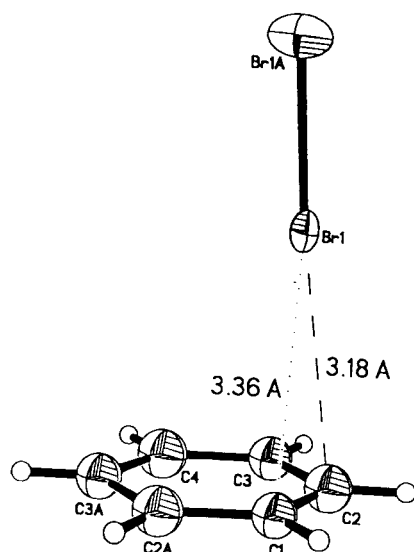
Such an obvious void is difficult to understand because the existence of metastable (prereactive) complexes in such common and diverse organic reactions as the Diels–Alder condensations, aromatic and olefinic brominations, etc. has been known from the earliest times.<sup>4–6</sup> From a *thermodynamics* point of view, it is convenient to dismiss the inclusion of preequilibrium complexes since they (usually) play limited roles in the overall energetics of the chemical transformation, and perhaps the same can

be said of their importance in defining the *kinetics*. However, the facile preorganization of the reactants can provide mechanistic insight from a *structural* point of view, as so fruitfully exploited by biochemists.<sup>7</sup> Thus, by invoking the principle of least motion,<sup>8</sup> we easily envisage how atomic movements within a structured (prereactive) complex can lead to a mechanistically viable transition-state structure.

#### I. Case in Point: Electrophilic Bromination of Benzene (and Toluene)

More than 60 years ago, Hildebrand and co-workers noted the characteristic color changes of iodine solutions immediately attendant upon the addition of various aromatic hydrocarbons.<sup>9</sup> These spectral observations were later extended to bromine and chlorine, and spectrophotometric analyses established the formation of [1:1] molecular complexes,<sup>10,11</sup> e.g., where X<sub>2</sub> = I<sub>2</sub>, Br<sub>2</sub>, Cl<sub>2</sub>, etc.

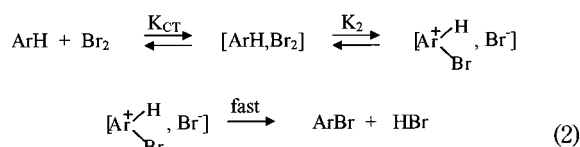




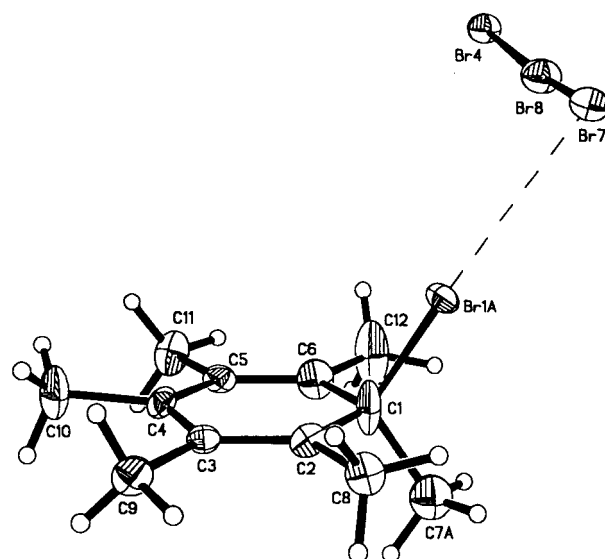
**Figure 1.** ORTEP diagram of the preequilibrium complex of benzene and bromine showing the pertinent charge-transfer  $\pi$ -bonding. Thermal ellipsoids of non-hydrogen atoms are shown at the 50% probability level.

The uniformly limited formation constants, typically with  $K_{CT} < 5 \text{ M}^{-1}$ , identified these as weak intermolecular complexes. Nonetheless, Hassel and Stromme in 1954 were able to obtain single crystals of the benzene complexes with bromine and chlorine (by controlled freezing of the pure components in glass capillaries) sufficient for X-ray crystallography at  $-50^\circ\text{C}$ .<sup>12</sup> Our recent refinement of their crystallography at lower temperatures reveals the *highly structured* preequilibrium complex shown in Figure 1,<sup>13</sup> in which the axially symmetric  $\text{Br}_2$  is poised specifically over a single (C–C) center of benzene. Moreover, the intermolecular (bromine) separation from the benzene plane is  $0.5 \text{ \AA}$  closer than that predicted by the van der Waals radii to establish the *inner-sphere* character of the noncovalent bonding of bromine in the metastable complex.<sup>14</sup> Its prereactive character is revealed by the spontaneous transformation of the crystalline  $[\text{C}_6\text{H}_6, \text{Br}_2]$  complex upon standing quantitatively into an equimolar mixture of bromobenzene and hydrogen bromide.<sup>15</sup> The further (structural) delineation of electrophilic aromatic bromination is provided by the isolation and X-ray crystallography of the  $\sigma$ -adduct or Wheland intermediate when benzene is replaced by hexamethylbenzene under similar reaction conditions (see Figure 2).<sup>16</sup> [Note that the highly unstable  $\sigma$ -adduct of benzene is unlikely to be isolated owing to its facile  $\alpha$ -proton loss.<sup>17</sup>] Such structural studies taken together provide an unequivocal pathway for electrophilic aromatic bromination in which the key steps are shown in Scheme 1.

**Scheme 1**

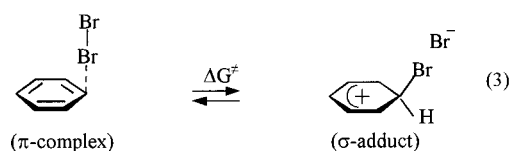


Most relevant to this study is the structural information provided by the preequilibrium  $\pi$ -complex in its transformation to the critical  $\sigma$ -adduct. Thus,



**Figure 2.** Molecular structure of the  $\sigma$ -adduct (or Wheland intermediate) derived from the bromine interaction with hexamethylbenzene to emphasize the least-motion transformation from the  $\pi$ -complex in Figure 1.

the composite of the ORTEP structures in Figures 1 and 2 represents a close to ideal least-motion study, i.e.

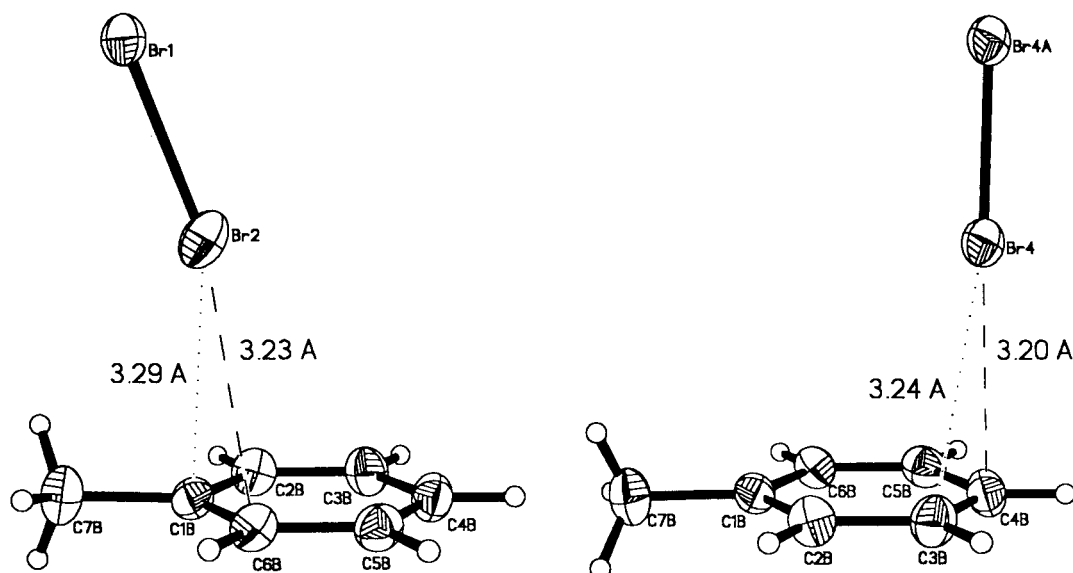


Even more striking is the regioselective transformation of the highly structured toluene  $\pi$ -complex with bromine situated specifically over the ortho and para positions in the crystal (see Figure 3) to afford the same isomeric (product) mixture of *o*- and *p*-bromotoluenes as that obtained in solution.<sup>18</sup> Although these preequilibrium intermediates are structurally akin to the (ordered) transition states for electrophilic bromination, it is important to emphasize that they are formed essentially upon bimolecular collision with no activation energy.<sup>19</sup> How can it be that two such states, so widely disparate in energy, can have structural features that bear so much in common? To address this question, we now turn to the electronic description of preequilibrium complexes to provide insight into the preorganization forces that bind the reactant pair.

## II. Mulliken's Quantitative Description of the Preequilibrium (Charge-Transfer) Complex

According to Mulliken, chemical compounds can be classified as either electron donors (D) or electron acceptors (A) in measure with their degree of electron-rich or electron-poor character.<sup>20,21</sup> Diffusive interaction of donors with acceptors spontaneously leads to their intermolecular complexation, in which the ground-state wave function ( $\Psi_{GS}$ ) derives from a linear combination of the principal van der Waals ( $\psi_{D,A}$ ) and dative ( $\psi_{D+A^-}$ ) contributions, i.e.<sup>22</sup>

$$\Psi_{GS} = a\psi_{D,A} + b\psi_{D+A^-} + \dots \quad (4)$$



**Figure 3.** Localized bonding specifically to the ortho (left) and para (right) centers of toluene in the preequilibrium (charge-transfer) complex with bromine.

The colors that are often observed with such electron-donor/-acceptor or EDA complexes arise from the electronic transition to the first excited state that is described by:

$$\Psi_{\text{ES}} = b\psi_{\text{D,A}} - a\psi_{\text{D+A}^-} + \dots \quad (4')$$

For weak complexes with the coefficients  $a \gg b$ , the electronic (charge-transfer) transition is tantamount to the photochemical conversion of the neutral (uncharged) ground state [D,A] to the dative (ion-pair) state  $[\text{D}^+, \text{A}^-]$ ; and it is commonly observed experimentally as the linear (Mulliken) correlation of the absorption maxima ( $h\nu_{\text{CT}}$ ) of the EDA complex with the ionization potentials (IP) of a series of related donors, i.e.,<sup>23</sup>

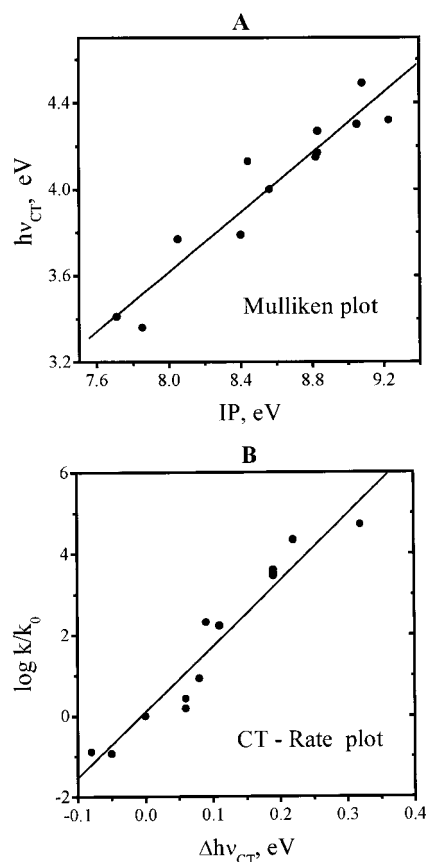
$$h\nu_{\text{CT}} = \text{IP} - \text{EA} + \text{constant} \quad (5)$$

when a common acceptor is employed [or vice versa for the electron affinities (EA) of a series of acceptors interacting with a common donor].<sup>24</sup>

As applied to the (weak) bromine complex of benzene in eq 1, the varying colors associated with the related complexation of different aromatic donors (ArH) follow the striking linear correlation shown in Figure 4A, as predicted by Mulliken.<sup>25</sup> Most noteworthy, however, is the linear correlation in Figure 4B of the CT transition energies ( $h\nu_{\text{CT}}$ ) with the second-order rate constants ( $\log k_{\text{Br}}$ ) for the electrophilic bromination of the same aromatic donors.<sup>26</sup> Such a remarkable linear correlation shows that those factors leading to the photoactivation ( $h\nu_{\text{CT}}$ ) of the EDA complex to the ion-radical pair  $[\text{ArH}^{\cdot+}, \text{Br}^{\cdot-}]$  are also pertinent to the attainment of the transition state ( $\log k_{\text{Br}}$ ) for the electrophilic aromatic substitution. We therefore conclude that an answer to our question lies in the charge-transfer character of the preequilibrium or electron donor/acceptor (EDA) complex.

### III. Charge-Transfer Character of the Preequilibrium (EDA) Complex

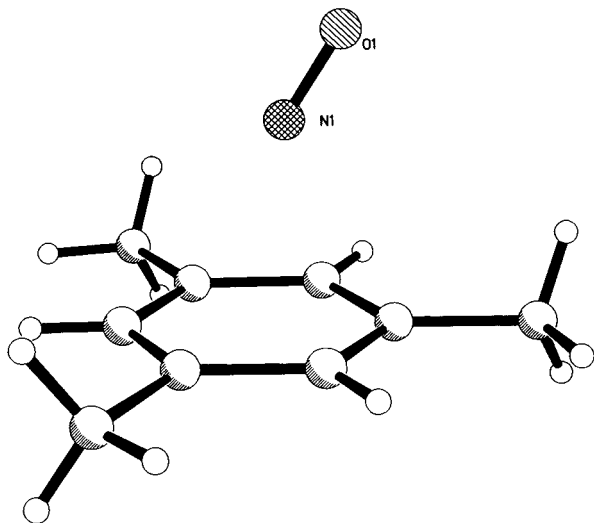
To assess quantitatively the changes in the charge-transfer character of the electron donor/acceptor complexes of various aromatic donors,<sup>27</sup> we now direct our



**Figure 4.** Charge-transfer energies ( $h\nu_{\text{CT}}$ ) of the preequilibrium complexes of bromine with various aromatic donors. (upper) Mulliken correlation with donor strength (IP) and the least-squares slope of 0.85. Lower figure is the rate correlation with the second-order rate constants ( $\log k_{\text{Br}}$ ) for electrophilic bromination with the least-squares slope of 0.94. (Selected data taken from Fukuzumi et al.<sup>26</sup>)

attention to those with the nitrosonium acceptor ( $\text{NO}^+$ ) for three principal reasons. First, as a simple





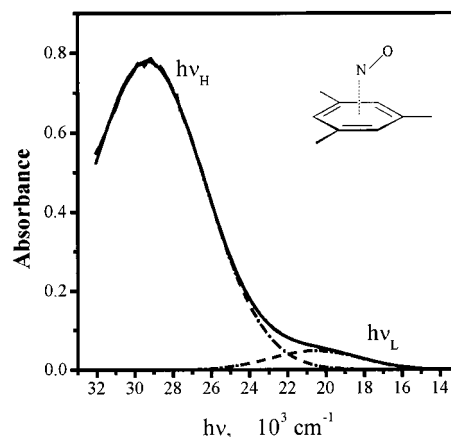
**Figure 5.** Molecular structure of the preequilibrium (charge-transfer) complex of mesitylene with the nitrosonium acceptor showing the typical  $\pi$ -bonding of  $\text{NO}^+$  atop the aromatic donor.<sup>28</sup>

diatomic the *partial* reduction of this cationic acceptor can be unambiguously measured by infrared spectroscopy of the N–O stretching frequency ( $\nu_{\text{NO}}$ ) and by X-ray crystallography of the N–O bond length, both of which undergo dramatic changes when  $\text{NO}^+$  ( $\nu_{\text{NO}} = 2272 \text{ cm}^{-1}$ ,  $r_{\text{NO}} = 1.06 \text{ \AA}$ ) is reduced to nitric oxide ( $\nu_{\text{NO}} = 1876 \text{ cm}^{-1}$ ,  $r_{\text{NO}} = 1.15 \text{ \AA}$ ).<sup>28</sup> Second, the nitrosonium cation has been identified as the active electrophile in aromatic nitrosation.<sup>29</sup> Third, nitrosonium salts can be pre-prepared as the pure (stable) salt  $\text{NO}^+\text{X}^-$  (where  $\text{X}^-$  represents poorly coordinating counterions such as  $\text{BF}_4^-$ ,  $\text{SbF}_6^-$ ,  $\text{SbCl}_6^-$ , etc.<sup>30</sup>) for quantitative study.

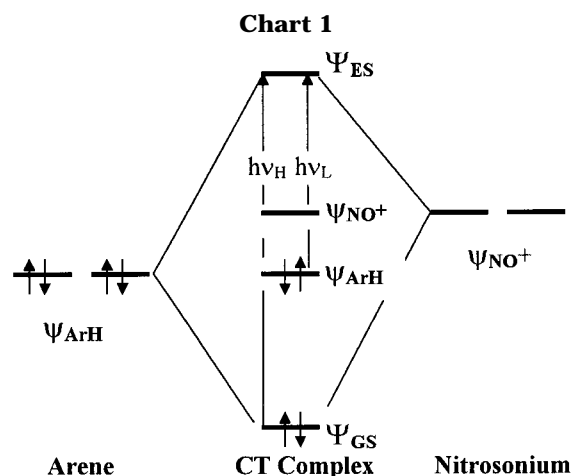
**A. Structural Changes upon Formation of the Preequilibrium Complex.** The spontaneous formation of the preequilibrium intermediate in eq 6 allows it to be isolated as bright cherry-brown crystals by mixing the components at low temperature ( $-78^\circ\text{C}$ ).<sup>32</sup> X-ray crystallography establishes the molecular structure of the  $[\text{ArH}, \text{NO}^+]$  complex in Figure 5 to be analogous to that of the bromine complex (Figure 1).<sup>31</sup> The inner-sphere character of this preequilibrium complex is apparent from the rather tight (noncovalent) binding of the acceptor to the aromatic donor, the NO separation from  $\text{ArH}$  being  $\sim 1 \text{ \AA}$  closer than that ordinarily allowed by the van der Waals radii.<sup>33</sup> [The latter is consistent with the large formation constant  $K_{\text{CT}}$  that can pertain in eq 6.<sup>34</sup>] More importantly, the N–O bond distance in the preequilibrium complex is substantially elongated (relative to that in the uncomplexed nitrosonium acceptor) and closely approaches that in the completely reduced (free) nitric oxide. Accompanying such a marked structural change is the expansion of the aromatic ring to that extant in the isolated aromatic cation radical.<sup>35</sup> Thus, from a strictly *structural* point of view, the nitrosonium acceptor upon its (reversible) complexation effectively suffers a one-electron reduction at the expense of the aromatic donor, i.e.,



How can it be that such an EDA complex (apparently constituted of the paramagnetic components  $\text{ArH}^{\bullet+}$  and



**Figure 6.** Typical charge-transfer (absorption) spectrum of the nitrosonium acceptor with aromatic donor (mesitylene), showing the Gaussian deconvolution into the high energy ( $h\nu_{\text{H}}$ ) and low energy ( $h\nu_{\text{L}}$ ) components.


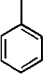
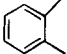
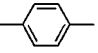
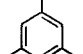
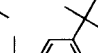
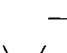
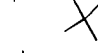
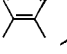
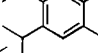
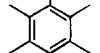
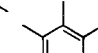


$\text{NO}^{\bullet}$ ) is completely ESR silent? To examine this question further, we turn to the electronic transitions in the preequilibrium complex.

**B. Charge-Transfer (Spectral) Absorptions in the Preequilibrium Complex.** The characteristic (yellow to cherry-brown) colors of the series of  $[\text{ArH}, \text{NO}^+]$  complexes derive from a pair of UV–vis absorption bands, typically illustrated in Figure 6. The intense, high energy band centered at  $\lambda \sim 340 \text{ nm}$  is more or less invariant with the aromatic donor strength ( $E_{\text{ox}}^{\circ}$ ),<sup>36</sup> but the weaker low-energy band  $\lambda_{\text{L}}$  varies linearly with  $E_{\text{ox}}^{\circ}$  in accord with the expectations of Mulliken theory.<sup>23</sup> This disparate (spectral) behavior of the two (charge-transfer) absorption bands leads to the orbital formulation of the donor/acceptor interaction of arene ( $\text{ArH}$ ) with  $\text{NO}^+$  presented in Chart 1.<sup>35</sup>

To describe the preequilibrium complex quantitatively, the mutual interaction of the donor/acceptor molecular orbitals is treated according to LCAO methodology,<sup>37,38</sup> in which only the frontier orbitals of the aromatic donor (HOMO) and the nitrosonium acceptor (LUMO) are explicitly taken into account.<sup>39</sup> In this formulation, the ground-state or bonding orbital  $\Psi_{\text{GS}}$  of the preequilibrium complex is represented as the linear combination of the donor and acceptor orbitals, i.e.,  $\Psi_{\text{GS}} = c_{\text{D}}\psi_{\text{D}} + c_{\text{A}}\psi_{\text{A}}$ , and likewise, the excited state or antibonding orbital is  $\Psi_{\text{ES}} = c_{\text{D}}'\psi_{\text{D}} + c_{\text{A}}'\psi_{\text{A}}$  (where the coefficients are normalized so that  $c_{\text{D}}^2 + c_{\text{A}}^2 = 1$  and  $c_{\text{D}}'^2 + c_{\text{A}}'^2 = 1$ ).<sup>40</sup> According to Chart

**Table 1. Typical Electron-Transfer Parameters for the Arene/Nitrosonium Redox Systems<sup>a</sup>**

Aromatic donor	$E_{\text{ox}}^0$ (V vs SCE)	$h\nu_{\text{H}}$ ( $10^3\text{cm}^{-1}$ )	$\Delta_{\text{AB}}$ (eV)	$H_{\text{AB}}$ (eV)	$\nu_{\text{NO}}$ ( $\text{cm}^{-1}$ )	$\epsilon_{\text{NO}}^2$
	2.7	29.80	1.22	1.74	2075	0.34
	2.42	29.57	0.94	1.77	2030	0.37
	2.13	29.77	0.65	1.82	2000	0.41
	2.06	30.16	0.58	1.85	1998	0.42
	2.11	29.51	0.63	1.80	1964	0.42
	2.01	29.38	0.53	1.80	1964	0.43
	1.83	29.51	0.35	1.87	1933	0.46
	1.81	30.11	0.32	1.82	b)	0.45
	1.75	30.11	0.27	1.86	1907	0.47
	1.62	30.14	0.14	1.87	1885	0.48
	1.59	29.51	0.11	1.83	1900	0.49
	1.50	28.94	0.02	1.79	1910	0.50

<sup>a</sup> From Rosokha et al. in ref 35. <sup>b</sup> Not measured.

1, the charge-transfer (spectral) absorptions are associated with a pair of electronic transitions from (i) the bonding MO ( $\Psi_{\text{GS}}$ ) to the antibonding MO ( $\Psi_{\text{ES}}$ ) and (ii) the nonbonding MO ( $\psi_{\text{ArH}}$ ) to the antibonding MO ( $\Psi_{\text{ES}}$ ) of the inner-sphere complex, as designated by  $h\nu_{\text{H}}$  (high energy band)<sup>40b</sup> and  $h\nu_{\text{L}}$  (low energy band), respectively, in Figure 6.<sup>41</sup> Application of the standard variation method leads to the energies of the ground and excited states as<sup>42</sup>

$$E_{\text{GS}} = (\epsilon_{\text{NO}} + \epsilon_{\text{ArH}})/2 - (\Delta_{\text{AB}}^2 + 4H_{\text{AB}}^2)^{1/2}/2 \quad (8)$$

$$E_{\text{ES}} = (\epsilon_{\text{NO}} + \epsilon_{\text{ArH}})/2 + (\Delta_{\text{AB}}^2 + 4H_{\text{AB}}^2)^{1/2}/2 \quad (9)$$

where the coulomb integrals ( $\epsilon_i = \int \psi_i H \psi_i$ ) represent the (one-electron) energies of the constituent donor and acceptor orbitals. The HOMO – LUMO gap or  $\Delta_{\text{AB}} = \epsilon_{\text{NO}} - \epsilon_{\text{ArH}}$  is evaluated experimentally as  $[E_{\text{ox}}^0(\text{ArH}) - E_{\text{red}}^0(\text{NO}^+)]$ , and the resonance integral  $H_{\text{AB}} = \int \psi_{\text{NO}} H \psi_{\text{ArH}}$  represents the donor/acceptor electronic interaction in the preequilibrium complex. Since the high-energy band arises via the electronic transition:  $\Psi_{\text{GS}} \rightarrow \Psi_{\text{ES}}$ , the transition energy derives from eqs 8 and 9 as:

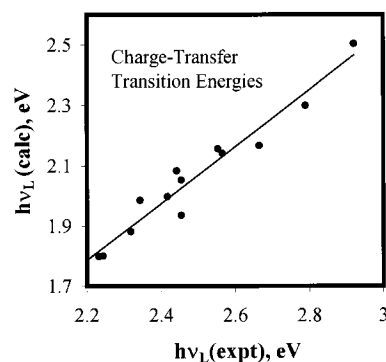
$$h\nu_{\text{H}} = E_{\text{ES}} - E_{\text{GS}} = (\Delta_{\text{AB}}^2 + 4H_{\text{AB}}^2)^{1/2} \quad (10)$$

The electronic coupling element in the inner-sphere complex is evaluated from eq 10 (by using the experimental values of  $\Delta_{\text{AB}}$  and  $h\nu_{\text{H}}$ ), and the sizable magnitudes of  $H_{\text{AB}}$  are listed in Table 1 for some representative aromatic donors.

According to the orbital diagram in Chart 1, the low energy (absorption) band corresponds to the transition:  $\psi_{\text{ArH}} \rightarrow \Psi_{\text{ES}}$ , and the transition energy can thus be evaluated directly from eq 9 as:

$$h\nu_{\text{L}} = (\Delta_{\text{AB}}^2 + 4H_{\text{AB}}^2)^{1/2}/2 + \Delta_{\text{AB}}/2 \quad (11)$$

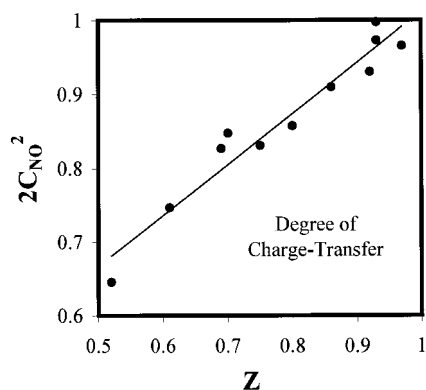
Figure 7 compares the experimental spectrum with the calculated spectrum from eq 11, and the solid line (with a slope of unity) thus confirms the validity of the LCAO–MO method to correctly predict the electronic changes in the preequilibrium complexes.<sup>43</sup>



**Figure 7.** Experimental validation of the theoretical (semi-empirical) methodology<sup>37,38</sup> according to eq 11 to correctly predict the experimental charge-transfer transition energies ( $h\nu_{\text{L}}$ ). The least-squares slope is 0.96.

**C. Charge-Transfer Structure of the Preequilibrium Complex.** The characteristic structural feature of





**Figure 8.** Experimental degree of charge transfer ( $Z$ ) in the preequilibrium complex as reflected in the theoretical (orbital) mixing coefficients  $C_{NO}^2$  in the ground-state wave function for various  $[ArH, NO]^+$  (least-squares slope is 0.71).

the inner-sphere complexes is their variable (X-ray) structures, which are also apparent from the monotonic variation of the N–O stretching frequencies with the aromatic donor strength.<sup>28</sup> Both measures reflect changes in the degree of electron transfer, hereinafter designated as  $Z$ . Since the acceptor is a simple diatomic, the IR changes in  $\nu_{NO}$  represent an unambiguous (experimental) measure of  $Z$ , i.e.,

$$Z = (\nu_{NO^+}^2 - \nu_{PC}^2) / (\nu_{NO^+}^2 - \nu_{NO}^2) \quad (12)$$

where the subscript  $NO^+$  refers to the uncomplexed nitrosonium cation, PC is the preequilibrium complex, and NO is the completely reduced (free) nitric oxide.

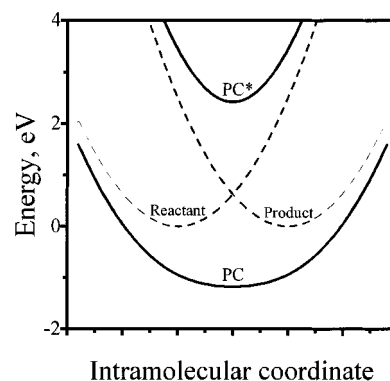
Theoretically, the degree of charge transfer can be viewed as the excess charge residing on the  $NO^+$  moiety in the inner-sphere complex. Such an electron excess in the ground-state complex is theoretically evaluated from the orbital coefficient as  $2C_{NO}^2$ ,<sup>44</sup> and the values of  $2C_{NO}^2$  calculated by the variation method are shown to be excellent measures of the experimental  $Z$  (see Figure 8). Importantly, the absolute magnitude of  $2C_{NO}^2$  is close to the experimental  $Z$ , especially for electron-rich arenes.

Since electron (charge) transfer from the arene to the complex orbital plays a major role in the stabilization, the energy gain during the preequilibrium complex formation is given by  $\Delta E_{PC} \cong E_{GS} - E_{ArH}$ , which with the aid of eq 8 is approximated as

$$\Delta E_{PC} \cong (\Delta_{AB}^2 + 4H_{AB}^2)^{1/2} - \Delta_{AB} \quad (13)$$

Equation 13 consists of two components: (1) the bonding/antibonding (orbital) splitting as given by  $E_{ES} - E_{GS}$  (see eq 10) and the HOMO – LUMO gap as given by  $\Delta_{AB}$ . Since  $4H_{AB}^2 \gg \Delta_{AB}^2$  (except in the endergonic limit, see Table 1), we conclude that  $\Delta E_{PC}$  and  $H_{AB}$  are strongly coupled—in other words, the *stabilization energy of the preequilibrium complex is largely dictated by the donor/acceptor interaction energy*, as also deduced from the structural changes determined by X-ray crystallography (see eq 7).<sup>45</sup> This conclusion predicts that  $H_{AB}$  also plays a major role in the experimental free energy change ( $\Delta G_{PC}$ ) and that maximum stabilization occurs at the isoenergetic potential at which the donor and acceptor strengths are comparable.

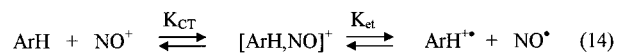
**D. Preequilibrium (Charge-Transfer) Complex and Electron Transfer.** The preorganizational associa-



**Figure 9.** Cross-section of the potential energy surface of the preequilibrium complex (PC) with the single minimum predicted by Marcus, Hush, and Sutin theory for class III electron-transfer reactions (with  $H_{AB} > \lambda/2$ ) and the charge-transfer transition to the excited state ( $PC^*$ ), i.e.,  $[PC] \rightarrow [PC^*]$  given by  $h\nu_{CT} = 2H_{AB}$ . For the arene/nitrosonium system in the isergonic region with the  $\Delta G_{ET}^0 = 0$  and  $\lambda_{CE} = 2.5$  eV for cross exchange in eq 14. The initial (reactant) diabatic state  $\{ArH + NO^+\}$  and final (product) diabatic state  $\{ArH^+ + NO\}$  are also quantitatively drawn to scale as the left and right dashed curves, respectively.<sup>50</sup>

tion of arene donors (ArH) with the nitrosonium acceptor is followed by electron transfer,<sup>35</sup> i.e., Scheme 2.

#### Scheme 2



The driving force for the overall electron transfer in eq 14 is given by

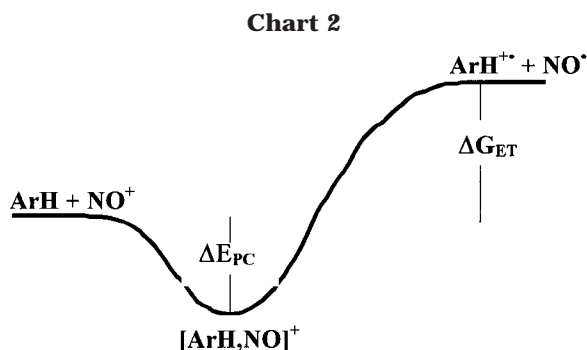
$$\Delta G_{ET} = F(E_{ox}^0 - E_{red}^0) \quad (15)$$

where  $F$  is the Faraday constant,  $E_{ox}^0$  represents the oxidation potential of the aromatic donor, and  $E_{red}^0 = 1.48$  V vs SCE is the reduction potential of nitrosonium acceptor. The dominant role of the preequilibrium complex as the key intermediate in the electron-transfer process between ArH and  $NO^+$  can be considered in the theoretical light of the Marcus–Hush formulation.<sup>46,47</sup> Owing to sizable magnitudes of the electronic coupling element ( $H_{AB}$ ) in the preequilibrium complex (see Table 1), the electron transfer in eq 14 must involve the inner-sphere mechanism.<sup>48</sup>

Let us now turn to Sutin's development of the Marcus–Hush formulation of various redox systems that specifically focuses on the magnitude of the electronic coupling element. In particular, Sutin considers two major (inner-sphere) mechanistic categories, class II and class III in which the limits of the electronic coupling element are as follows:  $H_{AB} > 200$  cm<sup>-1</sup> but less than  $\lambda_{CE}/2$  and  $H_{AB} > \lambda_{CE}/2$ , respectively, where  $\lambda_{CE}$  is the Marcus reorganization energy for the cross-exchange reaction.<sup>49</sup> Within this context, the value of  $\lambda_{CE}/2$  for the  $ArH/NO^+$  cross exchange can be obtained from their self-exchanges ( $ArH \rightleftharpoons ArH^+$  and  $NO^+ \rightleftharpoons NO$ ) as 1.2–1.3 eV, based on  $\lambda_{ArH} = 40$ –50 kcal mol<sup>-1</sup> and  $\lambda_{NO} = 69$  kcal mol<sup>-1</sup>.<sup>49b</sup> Since the magnitude of the electronic coupling of  $H_{AB} \sim 1.8$  eV is substantially larger than  $\lambda_{CE}/2$ , electron transfers from various arene donors to  $NO^+$  (as described in eq 14) clearly fall into class III. The energy surface for elec-

tron transfer consists of a single potential energy minimum—a typical cross-section of which is shown in Figure 9.<sup>50</sup>

Intermolecular electron-transfer reactions that belong to the class III category must occur with no activation energy. Chart 2 illustrates a profile of the potential energy surface that qualitatively depicts the free energy change along the reaction coordinate for the redox transformation of an arene/ $\text{NO}^+$  pair lying in a typical endergonic region of the driving force.<sup>51</sup>



In Chart 2, the inner-sphere complexes of arene donors with the nitrosonium acceptor are properly designated as  $[\text{ArH}, \text{NO}]^+$ , with the charge placed outside the brackets to emphasize the existence of only one potential energy minimum on the pathway from the  $\{\text{ArH} + \text{NO}^+\}$  reactants to the  $\{\text{ArH}^+ + \text{NO}^*\}$  products. As such, electron transfer is not a kinetics process but dependent on the thermodynamics in which electron redistribution is concurrent with complex formation, and the rate-limiting activation barrier is simply given by the sum of the energy gain from complex formation (eq 13) and the driving force for electron transfer (eq 15), i.e.,

$$\Delta G_{\text{ET}}^{\ddagger} = \Delta E_{\text{PC}} + \Delta G_{\text{ET}} \quad (16)$$

#### IV. Mechanistic Relevance of Preequilibrium (Charge-Transfer) Complexes to Arene Activation by $\text{NO}^+$ and $\text{NO}_2^+$ : Quantitative Comparison

Arene activation by nitrosonium cation ( $\text{NO}^+$ ), as depicted in Chart 2, has its counterpart with that by the nitronium cation ( $\text{NO}_2^+$ ). However, as structurally related as  $\text{NO}^+$  and  $\text{NO}_2^+$  may be, they differ markedly in their reactivity toward arene donors. Whereas benzene reacts with  $\text{NO}_2^+$  at essentially diffusion-controlled rates (to effect nitration),<sup>52</sup> the corresponding reactivity with  $\text{NO}^+$  under the same conditions (to effect nitrosation) is too slow to be measured.<sup>53</sup> (The latter occurs at measurable rates with only electron-rich arenes such as mesitylene, etc.<sup>29</sup>) Such divergent reactivity patterns of  $\text{NO}^+$  and  $\text{NO}_2^+$  are commonly evaluated by differences in their acceptor strengths and experimentally indicated by their reversible reduction potentials (compare eq 5).<sup>36</sup> However, the pertinent physical constants of  $\text{NO}^+$  and  $\text{NO}_2^+$  (Chart 3) are not strongly distinguished—their  $E^{\circ}_{\text{red}}$  values are reasonably comparable in different solvents. In fact, the only outstanding difference between  $\text{NO}^+$  and  $\text{NO}_2^+$  lies in the magnitude of the reorganization energies<sup>49</sup>— $\lambda_{\text{NO}_2}$  being more than twice  $\lambda_{\text{NO}}$  owing largely to the requisite

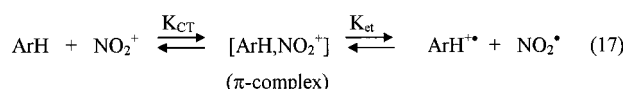
Chart 3

Structure	$\text{NO}_2^+$	$\text{NO}_2^*$	$\text{NO}^+$	$\text{NO}^*$
$r(\text{N-O}), \text{\AA}$	1.15	1.19	1.06	1.15
$\theta(\text{O-N-O}), \text{deg}$	175	134		
$f_s, \text{mdyne \AA}^{-1}$	17.4	11.0	23.9	15.9
$f_b, \text{mdyne \AA rad}^{-2}$	0.69	1.58		
Energy	$\text{NO}_2^+ / \text{NO}_2^*$		$\text{NO}^+ / \text{NO}^*$	
$E^{\circ}_{\text{red}}, \text{V vs Fc}$	1.03		1.00	
$\lambda, \text{kcal mol}^{-1}$	140		69	

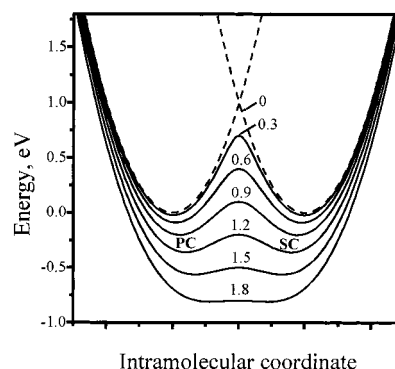
bending of  $\text{ONO}$  attendant upon the reduction of the almost linear (triatomic) cation.

To follow through with its comparison to  $\text{NO}^+$  as designated in eq 14 (Scheme 2), let us consider the corresponding electron-transfer process, viz. Scheme 3.

Scheme 3

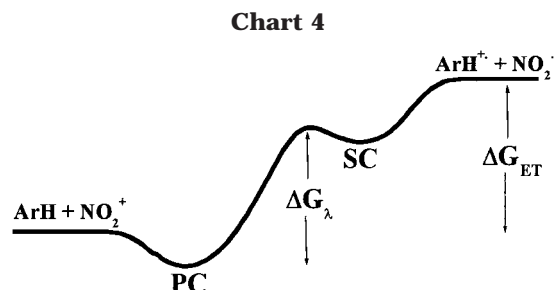


Since the temporal course of this electron transfer is not readily followed, owing to the high reactivity of  $\text{NO}_2^+$ , we now rely on the comparison of the physical constants in Chart 3 to draw some broad estimates of the electron coupling element for the preequilibrium intermediate in eq 17. If we take  $H_{\text{AB}}$  to be the same as that for  $\text{NO}^+$  (in eq 14) as a first approximation,<sup>54</sup> Sutin's treatment leads to the potential-energy profile shown in Figure 10<sup>55</sup> that consists of a double potential minimum (unlike that for  $\text{NO}^+$  in Figure 9) due to the reorganization energy of  $\lambda_{\text{NO}_2} = 140 \text{ kcal mol}^{-1}$ , which is roughly two times larger than  $\lambda_{\text{NO}}$ .<sup>49</sup> Figure 10 also includes the family of other energy profiles for  $\text{ArH}/\text{NO}_2^+$  pairs with progressively lower  $H_{\text{AB}}$  values. In each case, the single potential energy minimum characteristic of  $\text{ArH}/\text{NO}^+$  is replaced by double



**Figure 10.** Profiles of the potential energy surfaces (double minima) for the electron transfer in class II showing the progressive lowering of the activation barrier between the precursor complex (PC) and successor complex (SC) with increasing values of the electron-coupling element  $H_{\text{AB}}$ , as indicated (in eV). For the arene/nitronium redox system in the isergonic region, the initial (reactant) diabatic state  $\{\text{ArH} + \text{NO}_2^+\}$  and final (product) diabatic state  $\{\text{ArH}^+ + \text{NO}_2^*\}$  are quantitatively drawn to scale for  $\Delta G^{\circ}_{\text{ET}} = 0$  and  $\lambda_{\text{CE}} = 4.0 \text{ eV}$  for cross exchange in eq 17 in the dashed left and right dashed curves, respectively.<sup>55</sup>

potential energy minima. The latter consist of the separate precursor  $\pi$ -complex  $[\text{ArH}, \text{NO}_2^+]$  and the successor  $\pi$ -complex  $[\text{ArH}^+, \text{NO}_2^\bullet]$ , both with progressively shallower minima (and higher barriers that separate them) as the electron-coupling element  $H_{\text{AB}}$  decreases. In the limit with  $H_{\text{AB}} \approx 0$ , a single barrier separates the noninteracting reactant state  $\{\text{ArH} + \text{NO}_2^+\}$  and the product state  $\{\text{ArH}^+ + \text{NO}_2^\bullet\}$ . In other words, as a result of large  $\lambda_{\text{NO}_2}$ , electron transfer with  $\text{NO}_2^+$  cannot progress via a single preequilibrium  $\pi$ -complex like that with  $\text{NO}^+$  (Chart 3), and the typical cross-section of the potential energy surface shown in Chart 4 includes a pair of preequilibrium  $\pi$ -intermediates—designated PC and SC for precursor and successor complexes, respectively.

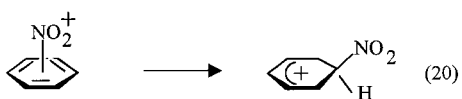
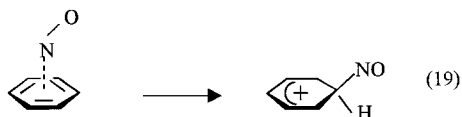


The difference between a potential-energy profile with a double minimum for  $\text{NO}_2^+$  (Chart 4) and that with a single minimum for  $\text{NO}^+$  (Chart 2) has important kinetic consequences. Indeed, *the rate of electron transfer to  $\text{NO}_2^+$  is significantly faster than that to  $\text{NO}^+$ , despite the large magnitude of  $\lambda_{\text{NO}_2}$  relative to  $\lambda_{\text{NO}}$* , since Chart 4 shows that the activation energy for overall electron transfer is simply given as<sup>56</sup>

$$\Delta G_{\text{ET}}^\ddagger = \Delta G_{\text{ET}} \quad (18)$$

### V. Comments on the Role of Preequilibrium Complexes in Electrophilic Aromatic Nitrosation versus Nitration via Electron Transfer

The preequilibrium formation of intermolecular charge-transfer complexes is common to both aromatic nitrosation and nitration, which are known to occur via the active electrophilic species  $\text{NO}^+$  and  $\text{NO}_2^+$ , respectively.<sup>57</sup> The interconversion of the  $\pi$ -complex to the  $\sigma$ -adduct (like that for bromination in eq 3) represents the critical activation step, i.e.,

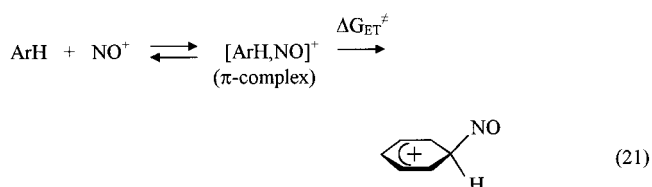


The least-motion study of such (direct or one-step) transformations cannot readily account for the fact that the  $\text{NO}_2^+$  moiety in eq 20 must overcome the sizable (reorganization) penalty for  $\text{ONO}$  bending (see Chart 3). Yet nitrations proceed at rates that are actually orders of magnitude faster than nitrosations,<sup>58</sup> in which the lower reorganization barrier for  $\text{NO}^+$  merely involves the simple N–O stretching mode (see Chart 3). Such a

significant reorganization obstacle is conceptually circumvented by decoupling the step involving reorganization from the step leading to the  $\sigma$ -adduct in both eqs 19 and 20. Indeed, electron-transfer activation as presented in Charts 2 and 4 for  $\text{NO}^+$  and  $\text{NO}_2^+$ , respectively, satisfies the two-step criterion since reorganization is implicit in electron transfer and it is separate from  $\sigma$ -adduct formation.

As applied to aromatic nitrosation, the activation process is as shown in Scheme 4, where the overall

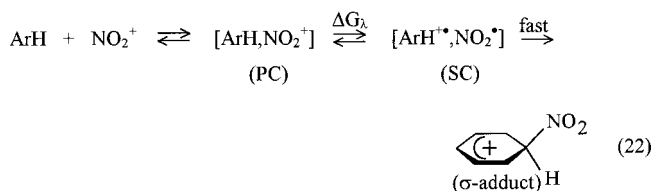
**Scheme 4**



activation barrier ( $\Delta G_{\text{ET}}^\ddagger$ ) is evaluated by eq 16.<sup>59</sup> Thus, the slow electron-transfer activation in eq 14 (coupled also with the subsequent slow deprotonation of the  $\sigma$ -adduct<sup>60</sup>) is responsible for aromatic nitrosations, which are by and large limited to only the most active (electron-rich) arene donors.<sup>61</sup>

The corresponding two-stage activation process for aromatic nitration via electron-transfer according to Chart 4 involves an additional intermediate -- the successor complex  $[\text{ArH}^+, \text{NO}_2^\bullet]$  which largely takes on the burden of the  $\text{NO}_2^+$  reorganization in the separate electron-transfer transformation of the precursor complex  $[\text{ArH}, \text{NO}_2^+]$ . The subsequent spontaneous collapse of the successor complex (SC) directly to the  $\sigma$ -adduct in Scheme 5 facilitates the electron-transfer pathway for nitration

**Scheme 5**

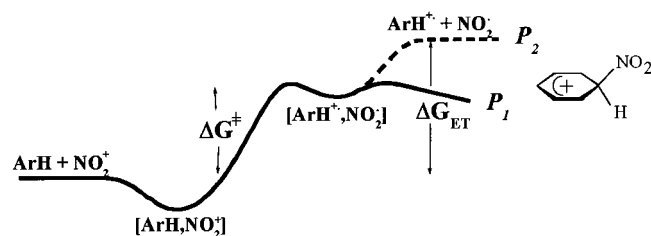


considerably<sup>62</sup> (Scheme 5) since it entirely bypasses the slow (energy-intensive) step leading from the successor complex  $[\text{ArH}^+, \text{NO}_2^\bullet]$  to the separated (noninteracting) ion-radical pairs  $\{\text{ArH}^+ + \text{NO}_2^\bullet\}$ , which is implicit in eq 18. The activation barrier for such a direct collapse of the ion-radical pair is substantially less than  $\Delta G_{\text{ET}}$  and leads to very fast nitration rates.<sup>64,65</sup> In the limit for nitrations involving preequilibrium complexation with small  $H_{\text{AB}}$  values, the rate will be limited by the  $\pi$ -interconversion of the precursor/successor complexes (i.e.,  $\Delta G_\lambda$ ) and not on the formation of the  $\sigma$ -adduct. The clear separation of the  $\pi$ -interconversion versus formation of the  $\sigma$ -adduct is illustrated in Chart 5.

Most importantly, the extent to which the  $\sigma$ -adduct is formed directly from the successor complex (pathway P<sub>1</sub>)<sup>67</sup> lowers the activation barrier relative to that for pathway P<sub>2</sub> (dashed curve) that formally proceeds via the free radical pair  $\{\text{ArH}^+ + \text{NO}_2^\bullet\}$ . Thus, Chart 5 underscores the caveat that the viability of electron-transfer mechanisms cannot be prejudged solely by



Chart 5



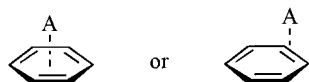
the free energy change for electron transfer ( $\Delta G_{ET}$ ), since the actual activation energy ( $\Delta G^\ddagger$ ) can be substantially less.

### Summary and Outlook

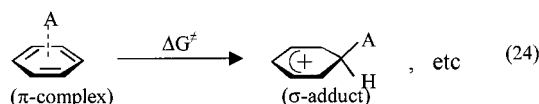
Metastable charge-transfer complexes are transiently observed as critical intermediates in electrophilic aromatic bromination and nitrosation with dibromine ( $\text{Br}_2$ ) and nitronium cation ( $\text{NO}^+$ ), respectively. Although structurally disparate,  $\text{Br}_2$  and  $\text{NO}^+$  nonetheless represent prototypical electron acceptors (A) that interact with various arenes as electron donors in a fast, initial equilibrium to form the [1:1] prereactive complex, i.e.,



As metastable as these preequilibrium complexes may be, transient (UV-vis) spectroscopic and low-temperature X-ray crystallographic analyses reveal their *highly structured*  $\pi$ -character as generically depicted below.<sup>31</sup>



In turn, these (ground-state)  $\pi$ -complexes are converted in a *rate-limiting* transformation to the  $\sigma$ -adduct, which is generally recognized<sup>17</sup> as the reactive intermediate leading to aromatic substitution, e.g.,

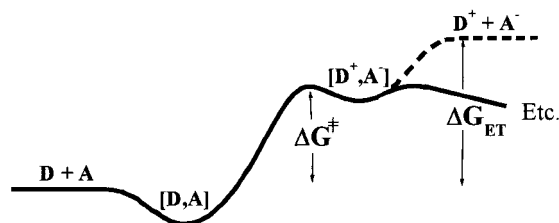


Although such a unimolecular transformation adheres to the least-motion principle, they involve intermediates that are highly disparate in energy—the ground-state  $\pi$ -complex being formed in a fast preequilibrium step, whereas the  $\sigma$ -adduct lies close to the rate-limiting transition state. The general question thus arises as to how a (low energy) ground-state structure such as the  $\pi$ -complex can take on the structure so close to the (high energy) transition state. This question comes into sharper focus when aromatic nitration with  $\text{NO}_2^+$  is considered in the light of aromatic nitrosation with  $\text{NO}^+$ . As related electrophiles,  $\text{NO}^+$  and  $\text{NO}_2^+$  have similar physical constants (see Chart 3) but differ markedly in their reorganization energy—the linear  $\text{NO}_2^+$  is heavily burdened by the bending penalty. As such, the direct (least-motion) formulation in eq 24 is not easily reconciled with the fact that  $\text{NO}_2^+$  is many orders of magnitude *more reactive* than  $\text{NO}^+$  in arene activation, despite its severe bending incurred in the attainment of the transition state. It is singularly important to note, however, that incorporation of the preequilibrium intermediate, con-

sisting of the reversible interchange between the precursor complex  $[\text{ArH}, \text{NO}_2^+]$  and the successor complex  $[\text{ArH}^+, \text{NO}_2^-]$  as shown in Chart 5, allows the reorganization barrier ( $\Delta G_i$ ) for  $\text{NO}_2^+$  to be clearly separated from the subsequent formation of  $\sigma$ -adduct.<sup>66</sup> By contrast, such an energetically favorable pathway is not available for  $\text{NO}^+$  (Chart 2) with consequent (substantially) slower rates for aromatic nitrosation.

The conclusion reached herewith underscores the general importance of the preequilibrium intermediate prior the reaction of any electron donor (D) with an electron acceptor (A). In particular, the emphasis on the charge-transfer character of the prereactive complex identifies the preorganization barrier to be a separate step from that leading to the transition-state structure. This important conclusion for organic-reaction mechanisms is identified in Chart 6 as the reorganizational (activation) barrier  $\Delta G^\ddagger$  that separates the precursor complex  $[\text{D}, \text{A}]$  from the successor complex  $[\text{D}^+, \text{A}^-]$ . In this way, electron-transfer mechanisms which hitherto may have been discounted owing to forbiddingly high endergonic driving forces (i.e.,  $\Delta G_{ET}$ ) can be accommodated.<sup>69</sup>

Chart 6



**Postscript.** Although we have deliberately restricted our attention in this Perspective to an in-depth study of the preequilibrium complexes pertinent to electrophilic aromatic bromination, nitrosation, and nitration, the prototypical free energy diagram, as outlined in Chart 6, should be viewed as a *general* mechanistic construct with universal applicability. Owing to the ubiquity of the charge-transfer phenomena,<sup>68</sup> we encourage further quantitative studies to provide experimental support for the viability of preequilibrium (precursor) complexes in the mechanistic elucidation of various types of other organic and organometallic reactions.

**Acknowledgment.** We thank the National Science Foundation and the R. A. Welch Foundation for financial support.

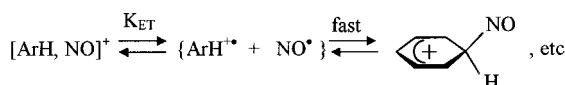
### References

- (1) For example, see: (a) Marcus, R. A. *Angew. Chem., Int. Ed. Engl.* **1993**, 32, 1111. (b) Sutin, N. *Acc. Chem. Res.* **1968**, 1, 255. (c) Morocuma, K. *Acc. Chem. Res.* **1977**, 10, 294.
- (2) (a) Scheiner, S., Ed. *Molecular Interaction. From van der Waals to Strongly Bound Complexes*; Wiley: New York, 1997. (b) Hobza, P.; Zahradnik R. *Intermolecular Complexes*; Elsevier: New York, 1988. (c) Ratajczak, H.; Orville-Thomas W. J. *Molecular Interaction*; Wiley: New York, 1980; Vol. 1. (d) See also the unusual number (3) of thematic issues of *Chem. Rev.* that have been issued in the last dozen years: viz. **1988** (Vol. 88), **1994** (Vol. 94), and **2000** (Vol. 100).
- (3) See, e.g.: Boyer, R. *Concepts in Biochemistry*; Brooks/Cole: Monterey, CA, 1999. See also: Gutman, F.; Johnson, C.; Keyzer, H.; Molnar, J. *Charge-Transfer Complexes in Biological Systems*; Dekker: New York, 1977.
- (4) (a) Pfeiffer, P.; Bottler, T. *Chem. Ber.* **1918**, 51, 1819. (b) Pfeiffer, P.; Jowleff, W.; Fischer, P.; Monti, P.; Mully, H. *Liebigs Ann.* **1916**, 412, 253. (c) Kuhn, R.; Wagner-Jauregg, T. *Ber. Dtsch. Chem. Ges.*, **1930**, 63, 2662. (d) Kuhn, R.; Wagner-Jauregg, T.

- Helv. Chim. Acta* **1930**, *13*, 9. (e) Klotzel, M. C. *Organic Reactions*; Wiley: New York, 1948; Vol. 4, p 9. (f) Woodward, R. B. *J. Am. Chem. Soc.* **1942**, *64*, 3058. (g) See also: Fukuzumi, S.; Kochi, J. K. *Tetrahedron* **1981**, *38*, 1035.
- (5) (a) Keefer, R.; Andrews, L. J. *J. Am. Chem. Soc.* **1950**, *72*, 4677. (b) Andrews, L. J.; Keefer, R. M. *Molecular Complexes in Organic Chemistry*; Holden-Day: San Francisco, 1964.
- (6) (a) Buckles, R. E.; Yuk, J. P. *J. Am. Chem. Soc.* **1953**, *75*, 3048. (b) Mayo, F. R.; Katz, J. J. *J. Am. Chem. Soc.* **1947**, *69*, 1339. (c) Dubois, J. E.; Garnier, F. *Spectrochim. Acta Part A*, **1967**, *23A*, 2279. (d) Fukuzumi, S.; Kochi, J. K. *J. Am. Chem. Soc.* **1981**, *103*, 2783.
- (7) Structural emphasis in biochemical mechanisms doubtlessly arises from the overriding concern for stereospecificity, which is not directly addressed by either a thermodynamics or kinetics treatment of reaction mechanisms. For some recent developments, see the thematic issue of *Chemical Reviews*: Ahn, N., Ed. *Chem. Rev.* **2001**, *101*, 2207.
- (8) Hine, J. J. *J. Org. Chem.* **1966**, *31*, 1236; *Adv. Phys. Org. Chem.* **1977**, *15*, 66.
- (9) (a) Pitzer, K. S.; Hildebrand J. H. *J. Am. Chem. Soc.* **1941**, *63*, 2472. (b) Benesi, H. A.; Hildebrand, J. H. *J. Am. Chem. Soc.* **1949**, *71*, 2703.
- (10) For a comprehensive review, see: Andrews, L. J.; Keefer, R. M. In ref 5b.
- (11) Fukuzumi, S.; Kochi, J. K. *J. Org. Chem.* **1981**, *46*, 4116.
- (12) (a) Hassel, O.; Strømme K. O. *Acta Chem. Scand.* **1958**, *12*, 1146. (b) Hassel, O.; Strømme K. O. *Acta Chem. Scand.* **1959**, *13*, 1781.
- (13) Vasilyev, A. V.; Lindeman, S. V.; Kochi, J. K. *J. Chem. Soc., Chem. Commun.* **2001**, 909.
- (14) Inner-sphere complexes involve the interpenetration of the coordination spheres of (donor/acceptor) components. See: Cotton, F. A.; Wilkinson G. *Advanced Inorganic Chemistry*, 5th ed.; Wiley: New York, 1988.
- (15) (a) Vasilyev, A. V.; Lindeman, S. V.; Kochi, J. K. *New J. Chem.*, in press. (b) This low-temperature observation is tantamount to the direct involvement of the charge-transfer complex in a chemical transformation. Compare: Kiselev, V. D.; Miller, J. G. *J. Am. Chem. Soc.* **1975**, *97*, 4036.
- (16) Hubig, S. M.; Kochi, J. K. *J. Org. Chem.* **2000**, *65*, 6807.
- (17) See: Taylor, R. *Electrophilic Aromatic Substitution*; Elsevier: New York, 1991.
- (18) De la Mare, P. B. D. *Electrophilic Halogenation*; Cambridge University Press: London, 1976.
- (19) A critical (kinetics) feature of preequilibrium complexes is their diffusive formation with (essentially) no activation barrier.<sup>24</sup>
- (20) Mulliken, R. S. *J. Am. Chem. Soc.* **1952**, *74*, 811
- (21) Mulliken, R. S.; Person, W. B. *Molecular Complexes*; Wiley: New York, 1969.
- (22) Note that the normalization relationship:  $a^2 + b^2 = 1$  is implicit.
- (23) The relationship in eq 5 is especially applicable to weak charge-transfer complexes in the gas phase where IP is the ionization potential of the donor and EA is the electron affinity of acceptor.<sup>19</sup> In solution, the corresponding relationship is approximated as  $h\nu_{CT} = E_{ox}^* - E_{red}^* + \text{constant}$  (eq 5') when the solvation energies of related species are roughly the same.
- (24) Foster, R. *Organic Charge-Transfer Complexes*; Academic: New York, 1969.
- (25) For the discussion of the Mulliken correlation, see: Hanna, M. W.; Lippert, J. L. *Mol. Complexes* **1973**, *1*, 2.
- (26) Fukuzumi, S.; Kochi, J. K. *J. Am. Chem. Soc.* **1982**, *104*, 7599.
- (27) (a) According to Mulliken,<sup>21</sup> the charge-transfer character of an electron donor/acceptor complex relates to the relative contributions of the no-bond and dative wave functions  $\psi_{D,A}$  and  $\psi_{D^+,A^-}$ , respectively, as given by orbital contributions  $a$  and  $b$  in eq 4. (b) Ground-state charge-transfer complexes with orbital coefficients  $a \gg b$  such as  $[\text{ArH}, \text{Br}_2]$  are weakly polarized to  $[\text{ArH}^+, \text{Br}_2^-]$ , whereas strong charge-transfer complexes with  $b \approx a$  such as  $[\text{ArH}, \text{NO}^+]$  have ground states that are strongly polarized to  $[\text{ArH}^+, \text{NO}^*]$ .
- (28) Kim, E. K.; Kochi, J. K. *J. Am. Chem. Soc.* **1991**, *113*, 4962.
- (29) Bosch, E.; Kochi, J. K. *J. Org. Chem.* **1994**, *59*, 5573.
- (30) (a) For clarity, the counterion is omitted hereinafter in the discussion. (b) For a recent review of nitrosonium complexes, see: Borodkin, G. I.; Shubin, V. G. *Russ. Chem. Rev.* **2001**, *70*, 211.
- (31) Detailed molecular structures of the various types of charge-transfer complexes of  $\pi$ -coordinated arenes are presented separately. See: Rosokha, S. V.; Kochi, J. K. In *Modern Arene Chemistry*; Astruc, D., Ed.; VCH: Weinheim, in press.
- (32) See Kim et al. in ref 28.
- (33) Bondi, A. J. *Phys. Chem.* **1964**, *68*, 441.
- (34) The formation constants of the preequilibrium complexes of  $\text{NO}^+$  are substantially larger than those of  $\text{Br}_2$  with the corresponding (arene) donors. Thus the  $[\text{ArH}, \text{NO}^+]$  complexes are considered to be strong, in contrast to  $[\text{ArH}, \text{Br}_2]$  complexes, which are weak.
- (35) (a) Rosokha, S. V.; Kochi, J. K. *J. Am. Chem. Soc.* **2001**, *123*, 8985. (b) Strictly speaking,  $\psi_{\text{ArH}}$  and  $\psi_{\text{NO}}$  in the precursor complex are both slightly perturbed (not shown).
- (36) Donor strength is conveniently measured as the ionization potential (IP, gas phase) or oxidation potential ( $E_{ox}^*$ , solution). Likewise, the acceptor strength is evaluated as the electron affinity (EA) or reduction potential ( $E_{red}^*$ ). See: Kochi, J. K. In *Comprehensive Organic Synthesis*; Trost, B. M., Fleming, I., Ley, S. V., Eds.; Pergamon: New York, 1991; Vol. 7, Chapter 7.4, p 849 ff.
- (37) The semiempirical LCAO–MO methodology is employed here since it provides a clear (orbital) description of the inner-sphere complex in terms of the donor/acceptor orbitals.
- (38) (a) Hückel, E. *Grundzüge der Theorie ungesättigter und aromatischer Verbindungen*; Verlag Chemie, G.m.b.H.: Berlin, 1938. (b) Flurry, R. L., Jr. *Molecular Orbital Theories of Bonding in Organic Molecules*; Marcel Dekker: New York, 1968. (c) Jorgensen, W. L.; Salem, L. *The Organic Chemist's Book of Orbitals*; Academic Press: New York, 1973. Dewar, M. J. S.; Dougherty, R. C. *The PMO Theory of Organic Chemistry*; Plenum Press: New York, 1975. (e) Carroll, F. A. *Perspectives on Structure and Mechanism in Organic Chemistry*; Brooks/Cole Publishing Co.: New York, 1998. For the application of MO–LCAO methodology to charge-transfer complexes, see: (f) Flurry, R. L. *J. Phys. Chem.* **1965**, *69*, 1927. (g) Flurry, R. L. *J. Phys. Chem.* **1969**, *73*, 2111. (h) Flurry, R. L. *J. Phys. Chem.* **1969**, *73*, 2787. Note that Flurry's approach cannot be used for calculation of MO energetics of the complexes under study, since he considered the extent of charge transfer to be constant in the series of complexes.
- (39) (a) Fleming, I. *Frontier Orbitals and Organic Chemical Reactions*; Wiley: New York, 1976. (b) Traven, V. F. *Frontier Orbitals and Properties of Organic Molecules*; Ellis Horwood: New York, 1992. (c) Klopman, G. *J. Am. Chem. Soc.* **1968**, *90*, 223. (d) Fukui, K. *Acc. Chem. Res.* **1971**, *4*, 57. (e) Fukui, K. *Angew. Chem., Int. Ed. Engl.* **1982**, *21*, 801.
- (40) (a) In the limit of complete charge transfer, this treatment is tantamount to the Mulliken formulation in eqs 4 and 4' where the coefficients  $a \approx b$ . (b) As such, the ground state of the  $[\text{ArH}, \text{NO}^+]$  complex involves the strong electronic coupling of  $\text{ArH}^+$  and  $\text{NO}^+$  and can be described in terms of two-electron delocalizations among the valence-bond forms:  $\{\text{ArH}, \text{NO}^+ \leftrightarrow \text{ArH}^+, \text{NO} \leftrightarrow \text{ArH}^{2+}, \text{NO}^-\}$ .
- (41) Although both transitions are allowed, the limited interaction of  $\psi_{\text{ArH}}$  with  $\Psi_{\text{ES}}$  (as determined by the transition moment  $\int \psi_{\text{ArH}}(\sigma) \Psi_{\text{ES}}$ ) results in an appreciably less intense low-energy band. See, e.g., Creutz et al. in ref 42.
- (42) Essentially the same basic form is obtained for the ground-state and excited-state energies by the two-state (electron-transfer) model based on the Mulliken formulation. See: Creutz, C.; Newton, M. D.; Sutin, N. *J. Photochem. Photobiol. A: Chem.* **1994**, *82*, 47.
- (43) This method also predicts the high energy transition ( $h\nu_{\text{H}}$ ) to be insensitive to the arene donor strength.
- (44) For the arene/ $\text{NO}^+$  donor/acceptor pair, the bonding molecular orbital is described as:  $\Psi_{\text{GS}} = c_{\text{ArH}}\psi_{\text{ArH}} + c_{\text{NO}}\psi_{\text{NO}}$ , where the normalization is  $c_{\text{ArH}}^2 + c_{\text{NO}}^2 = 1$ .
- (45) Note that ground-state perturbations ( $H_{\text{AB}}$ ) in weak aromatic (EDA) complexes with  $\text{Br}_2$  are too small to be detected as structural changes.
- (46) (a) Marcus, R. A. *J. Chem. Phys.* **1957**, *26*, 867. (a) Marcus, R. A. *Discuss. Faraday Soc.* **1960**, *29*, 21. (b) Marcus, R. A. *J. Phys. Chem.* **1963**, *67*, 853. (c) Marcus, R. A. *J. Chem. Phys.* **1965**, *43*, 679.
- (47) (a) Hush, N. S. Z. *Electrochem.* **1957**, *61*, 734. (b) Hush, N. S. *Trans. Faraday Soc.* **1961**, *57*, 557. (c) Hush, N. S. *Prog. Inorg. Chem.* **1967**, *8*, 391. (d) Hush, N. S. *Electrochim. Acta* **1968**, *13*, 1005.
- (48) For previous descriptions of the inner-sphere (electron-transfer) mechanism in organic processes, see: (a) Kochi, J. K. *Angew. Chem., Int. Ed. Engl.* **1988**, *27*, 1227. (b) Ebersson, L. *Electron-Transfer Reactions in Organic Chemistry*; Springer-Verlag: New York, 1987. (c) Ebersson, L.; Shaik, S. S. *J. Am. Chem. Soc.* **1990**, *112*, 4484. (d) Hubig, S. M.; Rathore, R.; Kochi, J. K. *J. Am. Chem. Soc.* **1999**, *121*, 617.
- (49) (a) For the self-exchange processes, the arene reorganization energy  $\lambda_{\text{ArH}}$  represents the activation energy required to change the nuclear (and electron) coordinates of  $\text{ArH}$  to those of  $\text{ArH}^+$  and, likewise, for  $\lambda_{\text{NO}}$  that required to change  $\text{NO}^+$  to  $\text{NO}$ . For the cross-exchange:  $\lambda_{\text{CE}} = (\lambda_{\text{NO}} + \lambda_{\text{ArH}})/2$ . (b) Ebersson, L.; Gonzalez-Luque, R.; Lorentzon, J.; Merchan, M.; Roos, B. O. *J. Am. Chem. Soc.* **1993**, *115*, 2898. (c) Lund, T.; Ebersson, L. *J. Chem. Soc., Perkin Trans. 2* **1997**, 1435. See also ref 48b.
- (50) According to Sutin,<sup>51b</sup> the dashed parabola on the left in the Figure 9 represents a cross-section of the diabatic potential energy surface of the *noninteracting* reactant pair, i.e.,  $\{\text{ArH} + \text{NO}^+\}$ , and that on the right represents the *noninteracting* product pair  $\{\text{ArH}^+ + \text{NO}^*\}$ . For the preequilibrium complex in Class III, the lower surface represents the broad single potential-energy well of the bonding state represented as  $[\text{ArH}, \text{NO}]^+$ , and the upper curve represents the antibonding (CT-excited) state  $[\text{ArH}^+, \text{NO}^*]^+$ . The energy difference between the minima of the

upper (antibonding) and lower (bonding) states is  $h\nu_H = 2H_{AB}$ . For simplicity, the redox system is represented with the isergonic driving force:  $\Delta G_{ET} = 0$ . (b) Sutin, N. *Prog. Inorg. Chem.* **1983**, 30, 441. See also: Sutin, N. *Adv. Chem. Phys.* **1999**, 106, 7. Brunschwig, B. S.; Sutin, N. *Coord. Chem. Rev.* **1999**, 187, 233.

- (51) (a) Note that the abscissa in Chart 2 (as well as in Charts 4 and 5, all drawn with the same endergonicity) is a composite representation of both intramolecular and intermolecular changes incurred upon electron transfer. The intramolecular changes involve bond lengths and angles as well as the electron-density distributions within the donor and the acceptor (as also depicted in Figures 9 and 10). Intermolecular changes relate to the separation/orientation of the donor/acceptor pair as well as the electron-density distribution relating to the bonding (2-electron) pair shown in Chart 1. (b) The strong electronic coupling of ArH and  $\text{NO}^+$ , as indicated by the enhanced values of  $H_{AB}$  in Table 1, accounts for (i) the two-electron bonding in the precursor complex and (ii) the absence of ESR activity.
- (52) Olah, G. A.; Malhotra, R.; Narang, S. C. *Nitration, Methods and Mechanisms*; VCH: New York, 1989.
- (53) Williams, D. L. H. *Nitrosation*; Cambridge: Cambridge University Press: 1988. Compare: Atherton, J. H.; Moodie, R. B.; Noble, D. R. *J. Chem. Soc. Perkin Trans. 2* **1999**, 699; **2000**, 229.
- (54) We hope that a collaborative interaction in progress (Professor Martin Head-Gordon) will provide high-level (theoretical) values of  $H_{AB}$  of use to further develop the potential energy surface of the arene/ $\text{NO}_2^+$  system.
- (55) (a) For clarity, Figure 10 (like Figure 9) is drawn according to Sutin<sup>50b</sup> for the class II redox pair in the isergonic region of the driving force. The diabatic curves are drawn with the reorganization energy of  $\lambda = 4.0$  eV and  $\Delta G_{ET}^{\circ} = 0$ . The various potential energy surfaces are drawn for the indicated values of  $H_{AB}$  (in eV). (b) Note that there is a continuous transition in the potential energy surfaces from single well (Figure 9) to double well (Figure 10) that is modulated by the magnitude of the electronic coupling element ( $H_{AB}$ ) relative to the reorganization barrier ( $\lambda/2$ ). Thus, the reaction profile for the ArH/ $\text{NO}^+$  system (class III) will progressively develop double-well character as  $H_{AB} = 1.8$  is gradually decreased to beyond  $H_{AB} < \lambda/2$  (1.2 eV), and conversely, the double-well predicted for the ArH<sub>2</sub>/ $\text{NO}_2^+$  system (Class II) will progressively evolve into a single-well surface as the electronic coupling element is gradually increased from  $H_{AB} = 1.8$  eV to  $H_{AB} > \lambda/2$  (2.0 eV). For a general discussion of this point, see Sutin in ref 50b.
- (56) For potential-energy surfaces with the activation energy for reorganization ( $\Delta G_i$ ) lying below the final state.
- (57) Hughes, E. D.; Ingold, C. K.; Reed, R. I. *Nature* **1946**, 158, 448, as reviewed in: Ingold, C. K. *Structure and Mechanism in Organic Chemistry*, 2nd ed.; Cornell: Ithaca, New York, 1969; pp 320 ff.
- (58) Challis, B. C.; Higgs, R. J.; Lawson, A. J. *J. Chem. Soc., Perkin Trans. 2* **1972**, 1831 and references therein.
- (59) The stepwise activation process for  $\Delta G_{ET}^{\circ}$  is:



Note that in this treatment, the energy of the pair of noninteracting radicals  $\{\text{ArH}^{\bullet+} + \text{NO}^{\bullet}\}$  is more or less equivalent to that of the  $\sigma$ -adduct, as previously established experimentally by their simultaneous observation via time-resolved spectroscopy. See: Hubig, S. M.; Kochi, J. K. *J. Am. Chem. Soc.* **2000**, 122, 8279.

- (60) To account for the sizable deuterium kinetic isotope effect in aromatic nitrosation (see Bosch et al. in ref 29).
- (61) Electron-rich arenes yield the most stable cation radicals, as indicated by their elevated values of  $K_{ET}$  (see ref 59).<sup>35</sup> Thus, the enhanced yields of arene cation radicals from electron-rich arenes will correlate with faster nitrosation rates.
- (62) (a) Independent time-resolved (ps) spectroscopic studies have established the facile (homolytic) coupling of the arene cation radical ( $\text{ArH}^{\bullet+}$ ) with  $\text{NO}_2^{\bullet}$  to form the  $\sigma$ -adduct—the second-order process of which occurs at diffusion-controlled rates. See: Kim, E. K.; Bockman, T. M.; Kochi, J. K. *J. Am. Chem. Soc.* **1993**, 115, 3091. (b) We note that the electron-transfer mechanism for aromatic nitration in Scheme 5 is a quantitative representation of the mechanism originally proposed by Perrin,<sup>62c</sup> in that the successor complex  $[\text{ArH}^{\bullet+}, \text{NO}_2^{\bullet}]$  and not the pair of (noninteracting) radicals  $\{\text{ArH}^{\bullet+} + \text{NO}_2^{\bullet}\}$  is considered to be the reactive intermediate. For the quantitative delineation of this (kinetic) distinction, see ref 63. (c) Perrin, C. L. *J. Am. Chem. Soc.* **1977**, 99, 5516.
- (63) (a) As depicted in Chart 4,  $\Delta G_{ET}$  represents the energy change for single electron transfer from the reactant diabatic state  $\{\text{ArH} + \text{NO}_2^{\bullet}\}$  to the separate product species, i.e., free  $\text{ArH}^{\bullet+}$  and free  $\text{NO}_2^{\bullet}$ . Bypassing the latter (see Chart 5) thus results in the lowering of the activation barrier (and in an increased rate) by an amount roughly relating to the electronic coupling element ( $H_{ab}$ ). (b) In a broader context in terms of electron-transfer mechanisms, the difference between the successor complex  $[\text{ArH}^{\bullet+}, \text{NO}_2^{\bullet}]$  and a pair of (more or less) free or noninteracting radicals  $\{\text{ArH}^{\bullet+} + \text{NO}_2^{\bullet}\}$  as the reactive intermediate in aromatic nitration is the *general* distinction between an *inner-sphere* and an *outer-sphere* process. See: Hubig S. M.; Rathore, R.; Kochi, J. K. *J. Am. Chem. Soc.* **1999**, 121, 617.
- (64) It is important to emphasize that the chemical behavior of the successor complex  $[\text{ArH}^{\bullet+}, \text{NO}_2^{\bullet}]$  in Class II is more like that of the free (noninteracting) radical pair  $\{\text{ArH}^{\bullet+}$  and  $\text{NO}_2^{\bullet}\}$ . The extent to which the  $\text{NO}_2^{\bullet}$  moiety in the successor complex is already (substantially) bent will further facilitate collapse to the  $\sigma$ -adduct. In this regard, the successor complex in class II systems is very different from the class III preequilibrium complex  $[\text{ArH}, \text{NO}]^+$ , which exhibits ion-radical behavior only upon separation to the free noninteracting  $\{\text{ArH}^{\bullet+}$  and  $\text{NO}^{\bullet}\}$  radical pair. (see Scheme 2).<sup>59</sup>
- (65) Furthermore, the subsequent deprotonation of the  $\sigma$ -adduct in aromatic nitration is rapid. See: (a) Melander, L. *Arkiv Kemi* **1950**, 2, 2111. (B) Melander, L. *Isotope Effects in Reaction Rates*; Ronald: New York, 1960.
- (66) The dichotomy between the *substrate reactivity* and *positional selectivity* in aromatic nitration with  $\text{NO}_2^+$  has been correctly addressed by Olah and co-workers<sup>52</sup> to the necessity of invoking (at least) two intermediates. According to our Scheme 5, such a mechanistic distinction results from the rate-limiting ( $\Delta G_i$ ) formation of the *successor complex*  $[\text{ArH}^{\bullet+}, \text{NO}_2^{\bullet}]^+$  which is formed in a completely separate step from the fast (ion-pair) collapse to the product-forming  $\sigma$ -adduct.
- (67) See the behavior of (class II) successor complexes, as described for nitration in footnote 60.
- (68) Compare: Rathore, R.; Kochi, J. K. *Adv. Phys. Org. Chem.* **2000**, 35, 193. See also: Foster, R. In ref 24. Andrews, L. J et al. In ref 5b.
- (69) Lund, T.; Ebersson, L. *J. Chem. Soc., Perkin Trans. 2* **1997**, 1435.

JO011072R